

A POINCARÉ-HOPF THEOREM FOR ORIENTED TRIANGULATED SURFACES VIA TILES

ETHAN D. BLOCH

ABSTRACT. The classical Poincaré-Hopf Theorem for smooth surfaces states that the sum of the indices of the zeros of a smooth vector field with isolated zeros on a compact smooth surface equals the Euler characteristic of the surface. We give a simple analog of the Poincaré-Hopf Theorem for orientable finite simplicial surfaces, where the vector fields are given via triangular tiles with a single arrow on each; in our version of the theorem, the index of such a discrete vector field is computed at every vertex of the simplicial surface. Our approach is inspired by the well-known analog of the Gauss-Bonnet Theorem for polyhedral surfaces.

1. INTRODUCTION

A well-studied polyhedral analog of a well-known theorem for smooth surfaces is the Gauss-Bonnet Theorem for polyhedral surfaces, which goes back at least as far as Descartes (see [Fed82]), and which is described very clearly in [Ban67, Ban70, DO11], among many others; this result has been generalized in various ways, for example in [CMS84, Blo98]. In the present note, we give a polyhedral analog of a different well-known theorem, the Poincaré-Hopf Theorem for smooth surfaces, which states that the sum of the indices of the zeros of a smooth vector field with isolated zeros on a compact smooth surface equals the Euler characteristic of the surface. Original references for the Poincaré-Hopf Theorem for smooth surfaces (and manifolds) are [Poi85, Hop26], and modern references may be found, for example, in [Mil65, Spi99]. There are various generalizations of the Poincaré-Hopf Theorem, including, among others, [Mor29, Pug68, Sch91, Sea08], and there are discrete versions on graphs such as [Kni12], but there does not appear to be a simple geometric analog of the Poincaré-Hopf Theorem for simplicial surfaces in the spirit of the polyhedral Gauss-Bonnet Theorem, which is based upon elementary calculations using angles; we give such an analog here in the orientable case.

The proof of our version of the Poincaré-Hopf Theorem, which is Theorem 14, is as simple as, and very similar to, the proof of the polyhedral Gauss-Bonnet Theorem, though our result also involves more preliminary definitions and lemmas than polyhedral Gauss-Bonnet, and leads to two additional theorems, with lengthier proofs, which have no analogs for polyhedral curvature.

2020 *Mathematics Subject Classification.* Primary 52B70; Secondary 57R25, 53A70.

Key words and phrases. Poincaré-Hopf Theorem, vector field, index, simplicial surface, tiling, Euler characteristic.

In our approach, polyhedral vector fields are given via triangular tiles with a single arrow on each. We compute the index of such a discrete vector field at every vertex of the simplicial surface and add all these indices, analogously to the polyhedral Gauss-Bonnet Theorem, where the curvature is computed at every vertex, and these curvatures are then added up.

Our discrete analogs of vector fields, and the definition of the index at each vertex, are defined in Section 2; our analog of the continuity of a vector field is in Section 3; our Poincaré-Hopf Theorem is in Section 4; we provide a much simpler way to compute the index of a vertex in Section 5; and in Section 6 we have two longer proofs.

We conclude this introduction with some assumptions and notation. Throughout this note we will restrict our attention to finite simplicial surfaces that are embedded in Euclidean space; different embeddings of combinatorially equivalent simplicial complexes will be considered as different simplicial complexes. Further, we will assume that all triangles in all simplicial surfaces are acute, and we will refer to such simplicial surfaces as **acute simplicial surfaces**.

Let K be a simplicial surface. If v is a vertex of K , we let $\text{star}(v, K)$ denote the star of v in K , and if σ is a triangle of K that has v as a vertex, we let $\alpha(v, \sigma)$ denote the angle at v in the triangle σ .

2. SIMPLEXWISE VECTOR FIELDS

In our polyhedral analog of a vector field on an acute simplicial surface in \mathbb{R}^n , rather than having a tangent vector at each point on the surface (which is not discrete, and has the problem of the lack of tangent planes at the vertices), we have one arrow for each triangle, where only certain triangles with arrows are allowed to meet in an edge.

Definition 1. Let K be an acute simplicial surface in \mathbb{R}^n .

- (1) Let σ be an acute triangle in K . A **simplex-arrow** for σ is an arrow in σ that has endpoints on the boundary of σ such each endpoint of the arrow is either the midpoint of an edge of σ or a vertex of σ , and the two endpoints are not contained in a single (closed) edge of σ .
- (2) A **simplexwise vector field** ϕ on K is an assignment of a simplex-arrow to each triangles in K , such that for every edge e of K , one of the following two conditions hold:
 - (i) the simplex-arrow in one of the triangles containing e ends at the midpoint of e , and the simplex-arrow in the other triangle containing e starts at the midpoint of e ;
 - (ii) neither of the simplex-arrows in the triangles containing e start or end at the midpoint of e , and the projections of both of these simplex-arrows onto the line containing the edge e are in the same direction.

△

Remark 2.

- (1) Up to linear transformation, including reflection, there are three types of triangles with simplex-arrows, as seen in Figure 1.

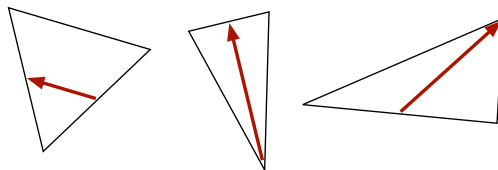


FIGURE 1.

(2) Up to linear transformation of each triangle, including reflection of both, there are 11 ways that two triangles with simplex-arrows in a simplexwise vector field can meet in an edge, as seen in Figure 2. \diamond

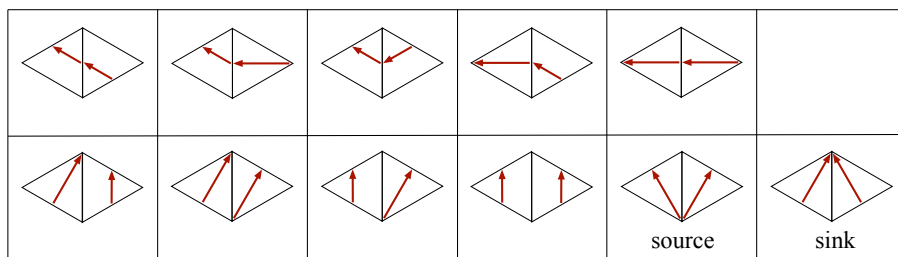


FIGURE 2.

Definition 3. The 11 pairs of adjacent triangles with simplex-arrows in Figure 2, up to linear transformation of each triangle, including reflection of both, are called the **allowable adjacencies** for a simplexwise vector field. The last two allowable adjacencies seen in the figure are called a **source** and a **sink**, respectively; the other (unnamed) allowable adjacencies are called **simple allowable adjacencies**. \triangle

See Figure 3 for examples of acute simplicial surfaces in \mathbb{R}^3 with simplexwise vector fields. The examples in Figure 3 are analogs of the smooth vector fields in Figure 4.

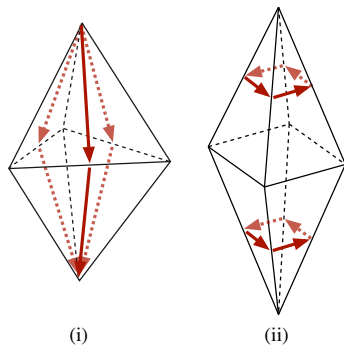


FIGURE 3.

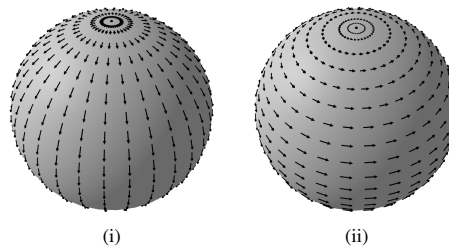


FIGURE 4.

We define the arrows in terms of their endpoints in the triangle, rather than simply associating to each triangle in \mathbb{R}^n a vector in \mathbb{R}^2 , because we will move our triangles via rotations and reflections, and we want the arrows to move with

the triangles. The endpoints of the arrows are limited to vertices or midpoints of edges because it is used in one proof, and there is no loss in that assumption. Only certain types of triangles with simplex-arrows can meet in an edge because that works well with the definition of continuity of simplexwise vector fields given in Section 3.

For our version of the Poincaré-Hopf Theorem, rather than computing the index at the zeros of a vector field, as in the smooth case, we will compute the index of a simplexwise vector field at each vertex of the acute simplicial surface. We start with some notation.

Definition 4. Suppose that two acute triangles with simplex-arrows in \mathbb{R}^n intersect in a common edge e , and let v be one of the vertices of e . Suppose further that the two triangles are given a coherent orientation. We can think of the two triangles as being in \mathbb{R}^2 , placed so that the orientation of the triangles matches the counterclockwise orientation of \mathbb{R}^2 . Let $\sigma_{v,e}^-$ and $\sigma_{v,e}^+$ be the triangle containing e that is clockwise and counterclockwise from e , respectively, as seen from the vertex v . Let $\alpha_{v,e}^-$ and $\alpha_{v,e}^+$ be the angles $\alpha(v, \sigma_{v,e}^-)$ and $\alpha(v, \sigma_{v,e}^+)$, respectively. Let $m_{v,e}^-$ and $m_{v,e}^+$ denote the simplex-arrows of the triangles $\sigma_{v,e}^-$ and $\sigma_{v,e}^+$, respectively. See Figure 5 for the various triangles and angles, and one possible example of the two simplex-arrows. \triangle

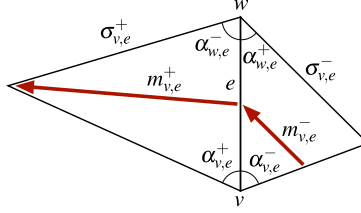


FIGURE 5.

In the following definition, which measures how the arrows change direction across an edge containing a vertex, and also in the subsequent definition of the index of a vertex, we need to choose an orientation for the star of the vertex; we will discuss the dependence upon the choice of orientation in Section 3.

Definition 5. Let K be an acute simplicial surface in \mathbb{R}^n with a simplexwise vector field ϕ . Let v be a vertex of K , and let e be an edge of K that has v as a vertex. Choose an orientation for $\text{star}(v, K)$.

The edge e is in the two triangles denoted $\sigma_{v,e}^-$ and $\sigma_{v,e}^+$. We can think of $\sigma_{v,e}^-$ and $\sigma_{v,e}^+$ as being in \mathbb{R}^2 , placed so that the orientation of the triangles matches the counterclockwise orientation of \mathbb{R}^2 . Let $R_{\alpha_{v,e}^-}(m_{v,e}^-)$ denote the simplex-arrow of the triangle with simplex-arrow that is the result of applying to the triangle $\sigma_{v,e}^-$ and its simplex-arrow the rotation of the plane counterclockwise around v by angle $\alpha_{v,e}^-$.

- (1) The pair v and e is **admissible** with respect to the chosen orientation of $\text{star}(v, K)$ if the vectors representing $R_{\alpha_{v,e}^-}(m_{v,e}^-)$ and $m_{v,e}^+$ are not negative multiples of each other.

- (2) If the pair v and e is admissible with respect to the chosen orientation of $\text{star}(v, K)$, the **vertex-edge turn** of e at v , denoted $\beta_{v,e}$, is the smaller angle from the vector representing $m_{v,e}^+$ to the vector representing $R_{\alpha_{v,e}^-}(m_{v,e}^-)$, where the angle is taken as positive if it is counterclockwise and as negative if it is clockwise; if the pair v and e is not admissible with respect to the chosen orientation of $\text{star}(v, K)$, then $\beta_{v,e}$ is not defined. \triangle

In Figures 6 (i) we see two triangles with simplex-arrows, and in Part (ii) of the figure we see the triangle $\sigma_{v,e}^-$ and its simplex-arrow rotated counterclockwise around vertex v by angle $\alpha_{v,e}^-$, where, as will be done throughout, the original triangles and simplex-arrows are shown solid with red arrows, and rotated triangles and simplex-arrows are shown dashed with green arrows. We see in Part (ii) of the figure that the edge of $\sigma_{v,e}^-$ that contains v and is not e will, as a result of the counterclockwise rotation around vertex v by angle $\alpha_{v,e}^-$, end up on top of e . Because the vectors representing $R_{\alpha_{v,e}^-}(m_{v,e}^-)$ and $m_{v,e}^+$ are not negative multiples of each other, as seen in Part (ii) of the figure, the pair v and e is admissible, and hence the vertex-edge turn $\beta_{v,e}$ is defined. In Part (iii) of the figure we see the arrows $m_{v,e}^+$ and $R_{\alpha_{v,e}^-}(m_{v,e}^-)$ translated so that they start at the same point, and we see $\beta_{v,e}$, which in this example is positive.

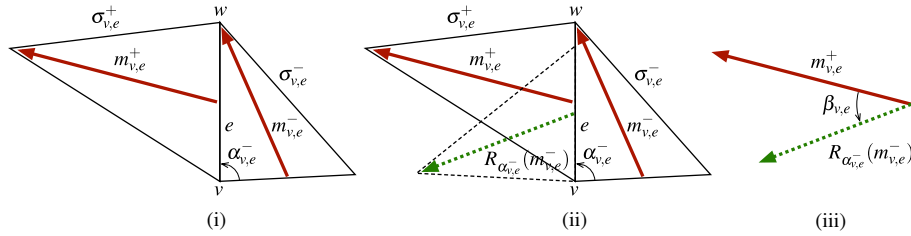


FIGURE 6.

In Figures 7 (i) we see a pair v and e that is not admissible, because, as seen in Part (ii) of the figure, the vectors representing $R_{\alpha_{v,e}^-}(m_{v,e}^-)$ and $m_{v,e}^+$ are negative multiples of each other; hence the vertex-edge turn $\beta_{v,e}$ is not defined.

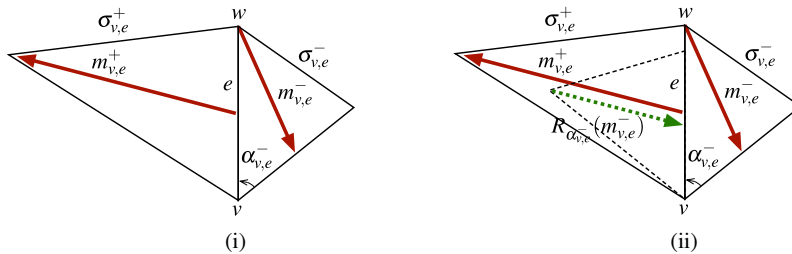


FIGURE 7.

The following definition is the global version of admissibility.

Definition 6. Let K be an acute simplicial surface in \mathbb{R}^n with a simplexwise vector field ϕ . The simplexwise vector field ϕ is **admissible** if for every vertex v of K , and every edge e of K that has v as a vertex, the pair v and e is admissible with respect to each of the two choices of orientation of $\text{star}(v, K)$. \triangle

We now define the index of a vertex with respect to a simplexwise vector field.

Definition 7. Let K be an acute simplicial surface with a simplexwise vector field ϕ , and let v be a vertex of K . Suppose that ϕ is admissible. Choose an orientation for $\text{star}(v, K)$. The **index** of v with respect to the simplexwise vector field, denoted $\text{ind}_v(\phi)$, is defined by

$$\text{ind}_v(\phi) = 1 - \frac{1}{2\pi} \sum_{e \ni v} \beta_{v,e}, \quad (1)$$

where the summation is over all the edges e of K that have v as a vertex. \triangle

For example, we use Equation (1) to compute the index of any of the vertices on the equator of the simplicial surface in Figure 3 (i), denoted v , where we choose the orientation for $\text{star}(v, K)$ obtained by looking at the simplicial surface from outside of it. We see in Figure 8 the result of taking each of the four edges containing v , starting at the edge above v and going counterclockwise, and flattening out the two triangles that contains the edge. Using the fact that all the triangles in this example are equilateral, it is straightforward to see that the four vertex-edge turns are $\frac{2\pi}{3}$, $\frac{\pi}{3}$, $\frac{2\pi}{3}$ and $\frac{\pi}{3}$, and hence $\text{ind}_v(\phi) = 1 - \frac{1}{2\pi} \left(\frac{2\pi}{3} + \frac{\pi}{3} + \frac{2\pi}{3} + \frac{\pi}{3} \right) = 0$.

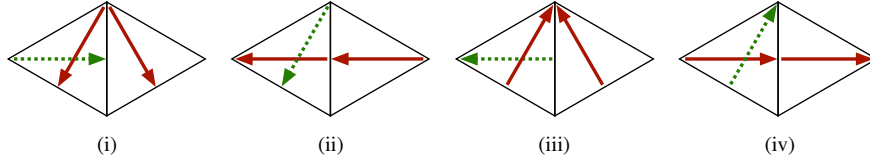


FIGURE 8.

The following lemma shows, as expected, that the index is always an integer.

Lemma 8. Let K be an acute simplicial surface with a simplexwise vector field ϕ , and let v be a vertex of K . Suppose that ϕ is admissible. Choose an orientation for $\text{star}(v, K)$. Then $\text{ind}_v(\phi)$ is an integer.

Proof. Let $\{e_1, e_2, \dots, e_n\}$ be the edges of K that have v as a vertex, in counterclockwise order. Let $i \in \{1, 2, \dots, n\}$. We use the abbreviations σ_i , m_i , α_i and β_i to denote σ_{v,e_i}^+ , m_{v,e_i}^+ , α_{v,e_i}^+ and β_{v,e_i} , respectively, as seen in the triangle on the left in Figure 9 (i). Let r_i be a vector starting at v in the direction of e_i , and let ε_i denote the counterclockwise angle from r_i to the vector representing m_i ; the angle ε_i is also seen in Part (i) of the figure.

In the three parts of Figure 9 we see how to compute the vertex-edge turn β_i , where in Part (i) of the figure we see the original two triangles with simplex-arrows, and in Part (ii) of the figure we see the triangle σ_{i-1} and its simplex-arrow rotated counterclockwise around vertex v by angle α_{i-1} . Observe that when the triangle

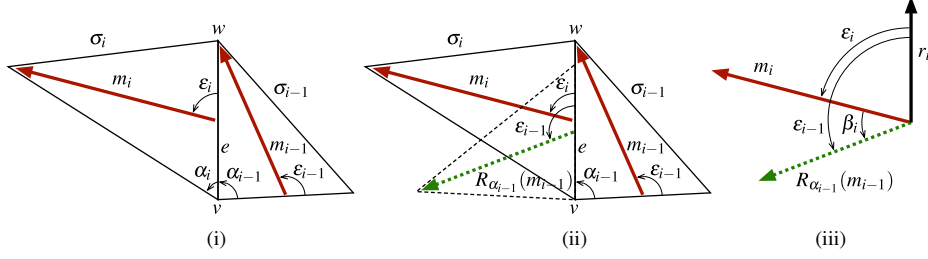


FIGURE 9.

σ_{i-1} is rotated, the bottom edge of this triangle is rotated so that it lands on the edge e_i , which means that the clockwise angle from r_i to the vector $R_{\alpha_{i-1}}(m_{i-1})$ equals the angle ϵ_{i-1} . In Part (iii) of the figure we see the arrows m_i , $R_{\alpha_{i-1}}(m_{i-1})$ and r_i translated so that they start at the same point, and we see ϵ_{i-1} , ϵ_i and β_i , where, as always, subtraction is mod n .

By definition, we know that β_i is the smaller angle (possibly clockwise or counterclockwise) from m_i to $R_{\alpha_{i-1}}(m_{i-1})$. We can find a formula for β_i in terms of ϵ_{i-1} and ϵ_i , as follows. There are three case to consider, as seen in the three parts of Figure 10, the first of which is from Figure 9.

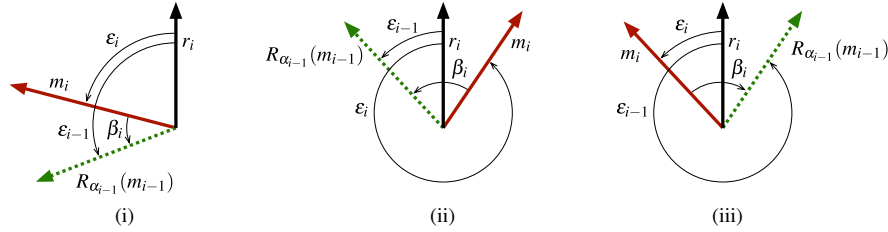


FIGURE 10.

First, suppose that the smaller angle from m_i to $R_{\alpha_{i-1}}(m_{i-1})$ does not contain a vector that is parallel to r_i , as in Figure 10 (i). We see that $\beta_i = \epsilon_{i-1} - \epsilon_i$.

Second, suppose that the smaller angle from m_i to $R_{\alpha_{i-1}}(m_{i-1})$ is counterclockwise and contains a vector that is parallel to r_i , as in Figure 10 (ii). We see that $\beta_i = 2\pi - (\epsilon_i - \epsilon_{i-1}) = \epsilon_{i-1} - \epsilon_i + 2\pi$.

Third, suppose that the smaller angle from m_i to $R_{\alpha_{i-1}}(m_{i-1})$ is clockwise and contains a vector that is parallel to r_i , as in Figure 10 (iii). We see that $-\beta_i = 2\pi - (\epsilon_{i-1} - \epsilon_i)$, and so $\beta_i = \epsilon_{i-1} - \epsilon_i - 2\pi$.

Putting the three cases together, we see that $\beta_i = \epsilon_{i-1} - \epsilon_i + w_i$, where w_i is one of 0, 2π or -2π .

Finally, we compute

$$\sum_{e \ni v} \beta_{v,e} = \sum_{i=1}^n \beta_i = \sum_{i=1}^n [\epsilon_{i-1} - \epsilon_i + w_i] = \sum_{i=1}^n \epsilon_{i-1} - \sum_{i=1}^n \epsilon_i + \sum_{i=1}^n w_i = \sum_{i=1}^n w_i.$$

It follows that $\sum_{e \ni v} \beta_{v,e}$ is a multiple of 2π , which implies $\text{ind}_v(\phi)$ is an integer. \square

3. CONTINUOUS ACUTE SIMPLICIAL SURFACE WITH SIMPLEXWISE VECTOR FIELD

Just as the Poincaré-Hopf Theorem in the smooth case requires smooth, and hence continuous, vector fields, so too in the present context we require a version of continuity for simplexwise vector fields. Examples show that without an assumption of continuity, our Poincaré-Hopf Theorem does not hold and our definition of the index of a vertex is not independent of the choice of orientation of the star.

The definition of a simplexwise vector field, which restricts which types of triangles with simplex-arrows can meet in an edge, is motivated by the idea of continuity, but it does not suffice for our proofs. Another intuitive idea of the continuity of a simplexwise vector field is that if the two triangles intersecting in the edge are placed in \mathbb{R}^2 , then the angle between the simplex-arrows in the two triangles (with no rotation) should be less than $\frac{\pi}{2}$, and that would suffice for some proofs, but it excludes an example we will need in the proof of Theorem 16, and which we will see shortly in Figure 11. As such, we will use a broader definition of continuity that is less intuitive, but which allows us to prove what we need.

Given that the index of a vertex is based upon the idea of a vertex-edge turn, defined in Definition 5 and which occurs at edges, it turns out that the notion of continuity that is useful to us here also occurs at the edges of the acute simplicial surface; a simplexwise vector field is continuous if it is continuous at every edge of K . For the following definition, observe that if e is an edge of an acute simplicial surface K with simplexwise vector field, and if the vertices of e are v and w , then $m_{w,e}^- = m_{v,e}^+$ and $m_{w,e}^+ = m_{v,e}^-$; for clarity, however, we will write these simplex-arrows both ways, as appropriate.

Definition 9. Let K be an acute simplicial surface with a simplexwise vector field ϕ . Let e be an edge of K . The simplexwise vector field ϕ is **continuous** at e if the following condition holds. Suppose that the two triangles containing e are given a coherent orientation. We can think of the two triangles as being in \mathbb{R}^2 , placed so that the orientation of the triangles matches the counterclockwise orientation of \mathbb{R}^2 . Let v and w be the vertices of e . The simplexwise vector field ϕ is defined to be continuous at e if the vectors in \mathbb{R}^2 representing each of the following four sets of three simplex-arrows is contained in an open half-plane (not necessary the same open half-plane for all the sets of three vectors):

- (a) $m_{v,e}^-, m_{v,e}^+$ and $R_{\alpha_{v,e}^-}(m_{v,e}^-)$;
- (b) $m_{w,e}^-, m_{w,e}^+$ and $R_{\alpha_{w,e}^-}(m_{w,e}^-)$;
- (c) $m_{v,e}^-, m_{v,e}^+$ and $R_{-\alpha_{v,e}^+}(m_{v,e}^+)$;
- (d) $m_{w,e}^-, m_{w,e}^+$ and $R_{-\alpha_{w,e}^+}(m_{w,e}^+)$.

The simplexwise vector field ϕ is **continuous** if it is continuous at every edge of K . △

In Figure 11, we see that the smaller angle between the two vectors representing $m_{v,e}^-$, and $m_{v,e}^+$ is greater than $\frac{\pi}{2}$, and yet the simplexwise vector field is nonetheless continuous at the edge e because the vectors representing $m_{v,e}^-$, and $m_{w,e}^+$, together

with any one of $R_{\alpha_{v,e}^-}(m_{v,e}^-)$, $R_{\alpha_{w,e}^-}(m_{w,e}^-)$, $R_{-\alpha_{v,e}^+}(m_{v,e}^+)$ or $R_{-\alpha_{w,e}^+}(m_{w,e}^+)$, are contained in an open half-plane, which is the criterion for continuity at e ; for visual ease, the various vectors have been translated so that they start at the origin, and have all been normalized to be unit vectors. Note that it is not required for continuity that the vectors representing $m_{v,e}^-$, and $m_{v,e}^+$ and all four of the rotated simplex-arrows are simultaneously in an open half-plane.

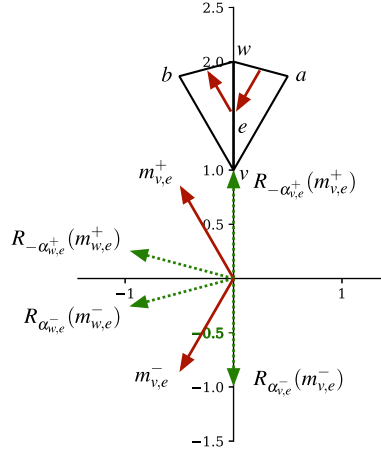


FIGURE 11.

In Figure 12 we see an edge e at which a simplexwise vector field is not continuous, where the various vectors have been translated and normalized as in the previous example. In this figure, we see, for example, that the vectors representing $m_{v,e}^-$, and $m_{v,e}^+$ and $R_{\alpha_{v,e}^-}(m_{v,e}^-)$ are not contained in an open half-plane, so that the simplexwise vector field is not continuous at e .

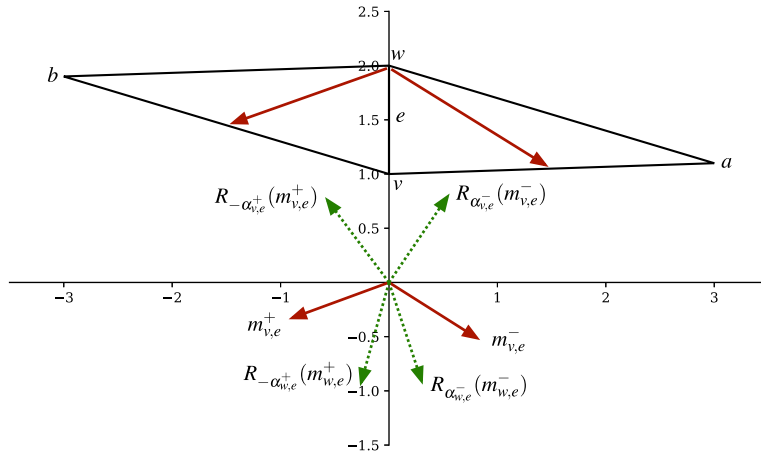


FIGURE 12.

The first part of the following remark is true because all triangles under consideration are acute, so the rotations used in the definition of continuity are always by

less than $\frac{\pi}{2}$, and the second part is true because when two vectors lie in an open half plane in \mathbb{R}^2 , they cannot be negative multiples of each other.

Remark 10. Let K be an acute simplicial surface with a simplexwise vector field ϕ .

- (1) Let e be an edge of K . Suppose that the two triangles containing e are given a coherent orientation. We can think of the two triangles as being in \mathbb{R}^2 , placed so that the orientation of the triangles matches the counterclockwise orientation of \mathbb{R}^2 . Let v a vertex of e . If the smaller angle between the two vectors in \mathbb{R}^2 representing the arrows $m_{v,e}^-$ and $m_{v,e}^+$ is less than or equal to $\frac{\pi}{2}$, then the simplexwise vector field ϕ is continuous at e . This condition is not if and only if, as seen in the example given in Figure 11.
- (2) If ϕ is continuous, then ϕ is admissible. ◇

We saw in the example given in Figure 12 that a simplexwise vector field need not be continuous at every edge, in spite of the restricted way in which triangles with simplex-arrows are allowed to meet in an edge in a simplexwise vector field. We now see that in fact most ways that two triangles with simplex-arrows can meet in an edge is continuous at that edge. Recall, as stated in Remark 2 (2), there are 11 allowable adjacencies up to linear transformation of each triangle, including reflection of both, of which two are a source and a sink, and the remaining ones of which are called simple allowable adjacencies. The following theorem says that a simplexwise vector field is always continuous in all cases other than sources and sinks; the proof of the theorem is in Section 6.

Theorem 11. *Let K be an acute simplicial surface with a simplexwise vector field ϕ , and let e be an edge of K . If the pair of triangles of K containing e is a simple allowable adjacency, then ϕ is continuous at e .*

We stress that verifying that the simple allowable adjacencies are all continuous relies upon the fact that for every triangle with a simplex-arrow, the endpoint of the arrow is either the midpoint of an edge or a vertex, but cannot be anywhere else in an edge. Examples show that the analogs of the simple allowable adjacencies, but allowing one of the simplex-arrows to have one endpoint that is in the interior of an edge but not at the midpoint, are not necessarily continuous.

In contrast to simple allowable adjacencies, a source or a sink might or might not be continuous at the common edge. For example, the simplexwise vector field seen in Figure 12, which is a source, is not continuous at e , as noted in the discussion of that figure; reversing the simplex-arrows in the two triangles would give a similar example that is a sink. On the other hand, as the reader can verify, a source and a sink where both triangles are equilateral are both continuous at the common edge.

Given that sources and sinks do not behave as nicely as the simple allowable adjacencies, it might be thought that sources and sinks should not be allowed in simplexwise vector fields, but, unfortunately, that is not possible if we want to be able to use simplexwise vector fields to create discrete analogs of smooth vector fields. For example, the simplexwise vector field in Figure 3 (i) is a discrete analog of the smooth vector field in Figure 4 (i), and in this simplexwise vector field the

two triangles containing every edge in the upper hemisphere form a source, and in the lower hemisphere they form a sink.

Though sources and sinks do not behave as nicely as the simple allowable adjacencies, we cannot disallow sources and sinks in simplexwise vector fields, because we want to be able to use simplexwise vector fields to create discrete analogs of smooth vector fields. For example, the simplexwise vector field in Figure 3 (i) is a discrete analog of the smooth vector field in Figure 4 (i), and in this simplexwise vector field the two triangles containing each edge in the upper hemisphere form a source, and in the lower hemisphere they form a sink.

4. POINCARÉ-HOPF THEOREM

We start with a lemma about vertex-edge turns.

Lemma 12. *Let K be an acute simplicial surface with a simplexwise vector field ϕ . Suppose that ϕ is continuous. Let e be an edge of K , and let v and w be the vertices of e . Choose a coherent orientations for $\text{star}(v, K)$ and $\text{star}(w, K)$. Let $\beta_{v,e}$ and $\beta_{w,e}$ denote the vertex-edge turns computed using the chosen orientation, and let $\hat{\beta}_{v,e}$ denote the vertex-edge turn computed using the reverse orientation.*

- (1) $\beta_{v,e} + \beta_{w,e} = \alpha_{v,e}^- + \alpha_{w,e}^-$.
- (2) $\hat{\beta}_{v,e} - \beta_{v,e} = \alpha_{v,e}^+ - \alpha_{v,e}^-$.

Proof. We can think of the two triangles containing e as being in \mathbb{R}^2 , placed so that the orientation of the triangles matches the counterclockwise orientation of \mathbb{R}^2 . See Figure 5 for the various angles, and one possible example of the two simplex-arrows.

Because ϕ is continuous, we know that there is an open half-plane in \mathbb{R}^2 that contains the vectors representing the arrows $m_{v,e}^-$, $m_{v,e}^+$ and $R_{\alpha_{v,e}^-}(m_{v,e}^-)$. There are then three possibilities for where $m_{v,e}^+$ is located in the plane in relation to $m_{v,e}^-$ and $R_{\alpha_{v,e}^-}(m_{v,e}^-)$, as seen in Figure 13; there appears to one more possible location of $m_{v,e}^+$ that is missing from the figure, but that case is not allowed because of continuity.

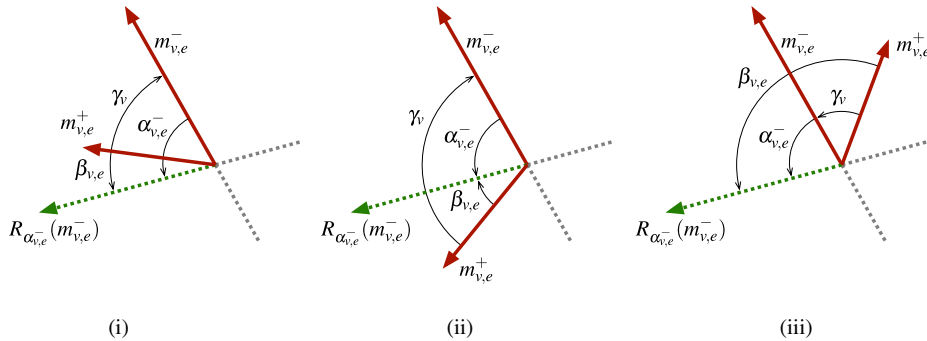


FIGURE 13.

Let γ_v be the smaller angle from $m_{v,e}^+$ to $m_{v,e}^-$, where, as usual, the angle is positive or negative depending upon whether it is counterclockwise or clockwise. In all

three parts of Figure 13, we see that $\beta_{v,e} = \alpha_{v,e}^- + \gamma_v$, where we use the fact that $\beta_{v,e}$ and γ_v can each be positive, negative or zero.

For Part (1) of this lemma, we observe that the same reasoning as above shows that $\beta_{w,e} = \alpha_{w,e}^- + \gamma_w$, where γ_w is the smaller angle from $m_{w,e}^+$ to $m_{w,e}^-$. Observing that $m_{w,e}^+ = m_{v,e}^-$ and $m_{w,e}^- = m_{v,e}^+$, we see that $\gamma_w = -\gamma_v$. It then follows that

$$\beta_{v,e} + \beta_{w,e} = (\alpha_{v,e}^- + \gamma_v) + (\alpha_{w,e}^- + \gamma_w) = \alpha_{v,e}^- + \alpha_{w,e}^-.$$

For Part (2) of this lemma, let k be the line that bounds an open half-plane in \mathbb{R}^2 containing the vectors representing the arrows $m_{v,e}^-$, $m_{v,e}^+$ and $R_{\alpha_{v,e}^-}(m_{v,e}^-)$; in the example seen in Figures 5 and 14, we can choose the line k to be the line containing the edge e , though that will not always be the case. Let T be the reflection of \mathbb{R}^2 in the line k . In Figure 14 we see the result of reflecting the two triangles in Figure 5 using the reflection T , where the reflected triangles, angles and arrows are denoted $\hat{\sigma}_{v,e}^-$, $\hat{\sigma}_{v,e}^+$, $\hat{\alpha}_{v,e}^-$, $\hat{\alpha}_{v,e}^+$, $\hat{m}_{v,e}^-$ and $\hat{m}_{v,e}^+$. We observe that $\hat{\alpha}_{v,e}^- = \alpha_{v,e}^+$, and $\hat{\alpha}_{v,e}^+ = \alpha_{v,e}^-$, and $\hat{m}_{v,e}^- = T(m_{v,e}^+)$ and $\hat{m}_{v,e}^+ = T(m_{v,e}^-)$.

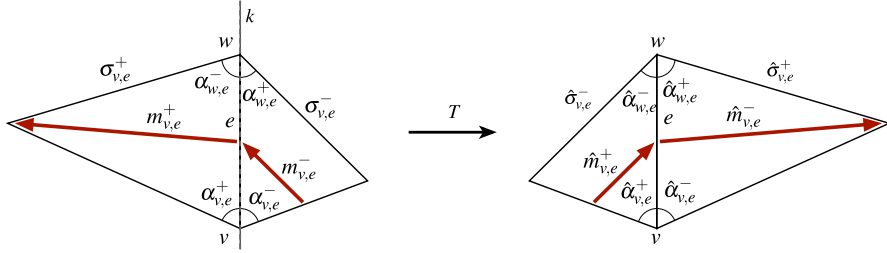


FIGURE 14.

The same reasoning as above shows that $\hat{\beta}_{v,e} = \hat{\alpha}_{v,e}^- + \hat{\gamma}_v$, where $\hat{\gamma}_v$ is the smaller angle from $\hat{m}_{v,e}^+$ to $\hat{m}_{v,e}^-$. Because $\hat{m}_{v,e}^+ = T(m_{v,e}^-)$ and $\hat{m}_{v,e}^- = T(m_{v,e}^+)$, and because the reflection T preserves angles but reverses orientation, we deduce that $\hat{\gamma}_v$ is the negative of the smaller angle from $m_{v,e}^-$ to $m_{v,e}^+$, so that that $\hat{\gamma}_v$ is the smaller angle from $m_{v,e}^+$ to $m_{v,e}^-$, which means $\hat{\gamma}_v = \gamma_v$. It then follows that

$$\hat{\beta}_{v,e} - \beta_{v,e} = (\hat{\alpha}_{v,e}^- + \hat{\gamma}_v) - (\alpha_{v,e}^- + \gamma_v) = \hat{\alpha}_{v,e}^- - \alpha_{v,e}^- = \alpha_{v,e}^+ - \alpha_{v,e}^-. \quad \square$$

We now resolve the question of the choice of orientation for the star of a vertex when computing the index in the case of a continuous simplexwise vector field.

Lemma 13. *Let K be an acute simplicial surface with a simplexwise vector field ϕ , and let v be a vertex of K . Suppose that ϕ is continuous. The index $\text{ind}_v(\phi)$ is independent of the choice of orientation for $\text{star}(v, K)$.*

Proof. Choose an orientation for $\text{star}(v, K)$. Let $\text{ind}_v(\phi)$ denote the index of v computed using the chosen orientation, and let $\widehat{\text{ind}}_v(\phi)$ denote the index of v computed using the reverse orientation.

Let $\{e_1, e_2, \dots, e_n\}$ be the edges of K that have v as a vertex, in counterclockwise order. Let $i \in \{1, 2, \dots, n\}$. We let β_{v,e_i} denote the vertex-edge turn computed using

the chosen orientation, and let $\hat{\beta}_{v,e_i}$ denote the vertex-edge turn computed using the reverse orientation. By Lemma 12 (2), we know that $\hat{\beta}_{v,e_i} = \beta_{v,e_i} + \alpha_{v,e_i}^+ - \alpha_{v,e_i}^-$. It follows that

$$\begin{aligned}
 \sum_{e \ni v} \hat{\beta}_{v,e} &= \sum_{i=1}^n \hat{\beta}_{v,e_i} \\
 &= \sum_{i=1}^n [\beta_{v,e_i} + \alpha_{v,e_i}^+ - \alpha_{v,e_i}^-] \\
 &= \sum_{i=1}^n \beta_{v,e_i} + \sum_{i=1}^n \alpha_{v,e_i}^+ - \sum_{i=1}^n \alpha_{v,e_i}^- \\
 &= \sum_{i=1}^n \beta_{v,e_i} + \sum_{i=1}^n \alpha_{v,e_i}^+ - \sum_{i=1}^n \alpha_{v,e_{i-1}}^+ \\
 &= \sum_{e \ni v} \beta_{v,e},
 \end{aligned}$$

where subtraction is mod n . We conclude that $\widehat{\text{ind}}_v(\phi) = \text{ind}_v(\phi)$. \square

Finally, we have our version of the Poincaré-Hopf Theorem. As is standard, we let V , E and F denote the number of vertices, edges and faces of a simplicial surface K , and we let $\chi(K)$ denote the Euler characteristic of K .

Theorem 14. *Let K be an acute simplicial surface with a simplexwise vector field ϕ . Suppose that K is orientable and ϕ is continuous. Then*

$$\sum_{v \in K} \text{ind}_v(\phi) = \chi(K),$$

where the summation is over all the vertices v of K .

Proof. Choose an orientation for K , which induces coherent orientations of the stars of all the vertices of K . We compute

$$\begin{aligned}
 \sum_{v \in K} \text{ind}_v(\phi) &= \sum_{v \in K} \left[1 - \frac{1}{2\pi} \sum_{e \ni v} \beta_{v,e} \right] \\
 &= V - \frac{1}{2\pi} \sum_{v \in K} \sum_{e \ni v} \beta_{v,e} \\
 &= V - \frac{1}{2\pi} \sum_{e \in K} \sum_{v \in e} \beta_{v,e} \\
 &= V - \frac{1}{2\pi} \sum_{e \in K} \sum_{v \in e} \alpha_{v,e}^-,
 \end{aligned}$$

where the last equality holds by Lemma 12 (1).

Next, we observe that every angle in every triangle in K is the angle $\alpha_{v,e}^-$ for precisely one vertex v and one edge e that has v as a vertex. Using the additional

fact that the sum of the angles in a triangle is π , it follows that

$$\begin{aligned}
 \sum_{v \in K} \text{ind}_v(\phi) &= V - \frac{1}{2\pi} \sum_{e \in K} \sum_{v \in e} \alpha_{v,e}^- \\
 &= V - \frac{1}{2\pi} \sum_{v \in K} \sum_{\sigma \ni v} \alpha(v, \sigma) \\
 &= V - \frac{1}{2\pi} \sum_{\sigma \in K} \sum_{v \in \sigma} \alpha(v, \sigma) \\
 &= V - \frac{1}{2\pi} \sum_{\sigma \in K} \pi \\
 &= V - \frac{1}{2}F.
 \end{aligned}$$

Finally, we note that in a simplicial surface it is always the case that $3F = 2E$, because every triangle has three edges, and every edge is in two triangles. Hence

$$\sum_{v \in K} \text{ind}_v(\phi) = V - \frac{1}{2}F = V - \frac{3}{2}F + F = V - E + F = \chi(K). \quad \square$$

We note that the above proof does not work in the non-orientable case.

5. SIMPLIFIED METHOD FOR COMPUTING THE INDEX OF A VERTEX

Our one remaining issue is that it is difficult to compute the index at a vertex by hand, because it involves measuring various angles in triangles, and rotating various vectors in the plane, all involving angles that are not always simple multiples of π . We now see a way of simplifying this type of calculations to the point where it can be done easily by hand, where the idea is that we can use equilateral triangles to compute the index of a vertex, even when the triangles in the acute simplicial surface are not equilateral.

To compute the index of a vertex v , we observe that given an orientation for $\text{star}(v, K)$, whereas there are only three types of triangles with simplex-arrows up to linear transformation, including reflection, as seen in Figure 1, if we consider triangles with simplex-arrows from the perspective of the vertex v , there are 12 different types, as seen in Figure 15.

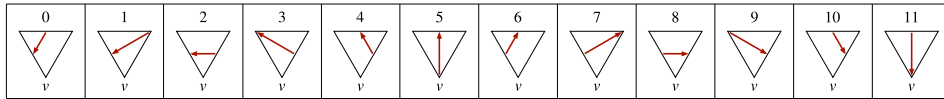


FIGURE 15.

Similarly, whereas there are only 11 ways that two triangles with simplex-arrows can meet in an edge up to linear transformation of each triangle, including reflection of both, as seen in Figure 2, if we consider such triangles from the perspective of the vertex v , there are 36 different ways two such triangles can meet in an edge,

as seen in Figure 16. The ordered pair associated with each pair of triangles consists of the numbers (from Figure 15) of the two triangles in clockwise order, and the additional number listed for each pair of triangles is the vertex-edge turn $\beta_{v,e}$ computed using equilateral triangles (the use of which will become apparent soon).

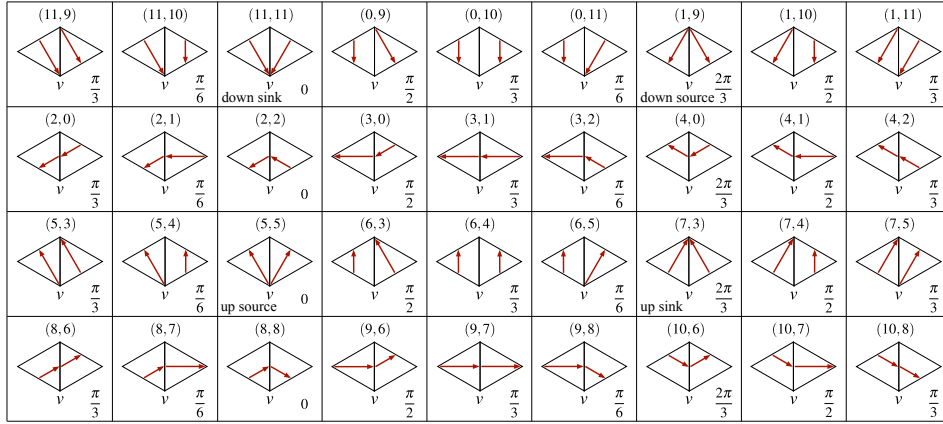


FIGURE 16.

Definition 15. Let K be an acute simplicial surface with a simplexwise vector field ϕ , and let v be a vertex of K . Choose an orientation for $\text{star}(v, K)$.

- (1) Let σ be a triangle with simplex-arrow of K that has v as a vertex. The **tile number** of σ at v is the number corresponding to the equivalent triangle with simplex-arrow using an equilateral triangle, with matching orientation, given in the chart in Figure 15.
- (2) Let $\sigma_1, \dots, \sigma_p$ be the triangles with simplex-arrows of K that have v as a vertex, listed in clockwise order corresponding to the orientation of $\text{star}(v, K)$. The **clockwise tile list** around v is the list $[a_1, a_2, \dots, a_p]$, determined up to cyclic permutation, of the tile numbers of $\sigma_1, \dots, \sigma_p$, starting at any choice of a triangle with simplex-arrow.
- (3) Among the configurations in Figure 16, the two sources (5, 5) and (1, 9) are called an **up-source** and a **down-source**, respectively, and the two sinks (7, 3) and (11, 11) are called an **up-sink** and a **down-sink**, respectively.

△

The following theorem gives a very easy way to compute the index at a vertex of a continuous simplexwise vector field without measuring angles in triangles and between vectors. The proof of the theorem is in Section 6.

Theorem 16. *Let K be an acute simplicial surface with a simplexwise vector field ϕ , and let v be a vertex of K . Suppose that ϕ is continuous. Choose an orientation for $\text{star}(v, K)$. Let $[a_1, a_2, \dots, a_p]$ be the clockwise tile list around v . The index of v is determined by the clockwise tile list $[a_1, a_2, \dots, a_p]$ alone, where Equation 1 is used with vertex-edge turns computed using the chart in Figure 16, as if all the triangles in $\text{star}(v, K)$ were equilateral.*

We use Theorem 16 to compute the index any of the vertices, denoted v , on the equator of the acute simplicial surface with simplexwise vector field in Figure 3 (ii), which does not have equilateral triangles. In Figure 17 we see a flattened version of $\text{star}(v, K)$, which has clockwise tile list is $[0, 10, 6, 4]$. This list gives rise to four pairs of adjacent tiles, again in clockwise order, which are $(0, 10)$, $(10, 6)$, $(6, 4)$ and $(4, 0)$. Using the chart in Figure 16, we obtain, respectively, the vertex-edge turns $\frac{\pi}{3}$, $\frac{2\pi}{3}$, $\frac{\pi}{3}$ and $\frac{2\pi}{3}$, and using Equation (1), we compute $\text{ind}_v(\phi) = 1 - \frac{1}{2\pi} \left(\frac{\pi}{3} + \frac{2\pi}{3} + \frac{\pi}{3} + \frac{2\pi}{3} \right) = 0$.

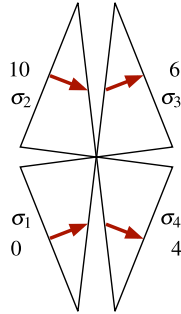


FIGURE 17.

6. PROOFS OF TWO THEOREMS

Proof of Theorem 11. Suppose that the pair of triangles of K containing e is a simple allowable adjacency. To show that ϕ is continuous at e is a matter of checking each of the nine cases shown in Figure 2, though at present we need to consider all possible acute triangles, not only the equilateral triangles seen in the figure. We will consider two of these nine cases, leaving to the reader the other cases, which are similar.

Without loss of generality, we assume that the vertices of the edge e are $v = (0, 0)$ and $w = (0, 1)$. The third vertices of the triangles to the left and right of e are denoted a and b , respectively. Because all triangles under consideration are acute, then a and b each has y -coordinate strictly between 0 and 1, and both points are outside the circle of radius $\frac{1}{2}$ centered at the midpoint of edge e ; see Figure 18, which shows two possibilities for a , but labels only one possible $m_{v,e}^+$ to avoid clutter.

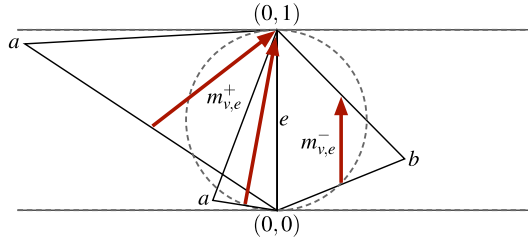


FIGURE 18.

The first case we consider is on the left of the bottom row of Figure 2, and is also seen in Figure 18. We observe that by the definition of triangles with simplex-arrows, the endpoints of $m_{v,e}^-$ are both at midpoints of edges, which means that the vector representing $m_{v,e}^-$ is in the direction of the positive y -axis. By looking at the extreme cases for $m_{v,e}^+$, which occurs on the one hand when a has y -coordinate close to 1 and x -coordinate very far in the negative direction, and on the other hand when a has both x -coordinate and y -coordinate close to 0, we see that the vector representing $m_{v,e}^+$ can be any vector ending in the interior of the first quadrant. As such, we see that the smaller angle between the vectors in representing $m_{v,e}^-$ and $m_{v,e}^+$ is less than $\frac{\pi}{2}$, and it follows from Remark 10 (1) that the simplexwise vector field ϕ is continuous at e .

The other three cases in the bottom row of Figure 2 other than the source and the sink are similar to the above case, and we omit the details.

The second case we consider is in the middle of the top row of Figure 2, and is also seen in each of the parts of Figure 19, where to avoid clutter the dashed lines and circle in Figure 18 are not shown here, but the same restrictions on a and b still apply. By looking at extreme cases (which are not shown in Figure 19), we see that the vector representing $m_{v,e}^-$ can be any vector ending in the interior of the third quadrant, and the vector representing $m_{v,e}^+$ can be any vector ending in the interior of the second quadrant. The smaller angle between the two vectors representing $m_{v,e}^-$ and $m_{v,e}^+$ is not necessarily less than $\frac{\pi}{2}$, and so we cannot use Remark 10 (1) in this case. Rather, we consider each of the other four vectors involved in the four parts of the definition of continuity, as seen in the four parts of Figure 19. In each part of this figure we see one of the other four vectors shown dashed; to avoid clutter, the simplex-arrows $m_{v,e}^-$ and $m_{v,e}^+$ are not labeled, but, as usual, are shown solid.

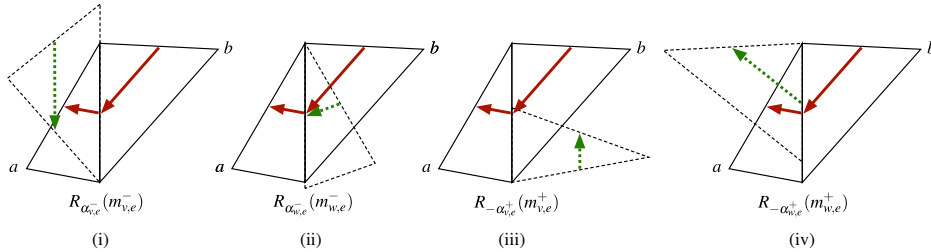


FIGURE 19.

First, as seen in Figure 19 (i), the vector representing $R_{\alpha_{v,e}^-}(m_{v,e}^-)$ is in the direction of the negative y -axis. It follows that the vectors representing all three of $m_{v,e}^-$, $m_{v,e}^+$ and $R_{\alpha_{v,e}^-}(m_{v,e}^-)$ are in an open half-plane bounded by a line obtained by rotating the y -axis about the origin counterclockwise very slightly.

Second, as seen in Figure 19 (ii), the vector representing $R_{\alpha_{w,e}^-}(m_{v,e}^-)$ can be any vector ending in the interior of the third quadrant. It follows that the vectors representing all three of $m_{v,e}^-$, $m_{v,e}^+$ and $R_{\alpha_{w,e}^-}(m_{v,e}^-)$ are in the open half-plane to the left of the y -axis.

Third, as seen in Figure 19 (iii), the vector representing $R_{-\alpha_{v,e}^+}(m_{v,e}^+)$ is in the direction of the positive y -axis. It follows that the vectors representing all three of $m_{v,e}^-$, $m_{v,e}^+$ and $R_{-\alpha_{v,e}^+}(m_{v,e}^+)$ are in an open half-plane bounded by a line obtained by rotating the y -axis about the origin clockwise very slightly.

Fourth, as seen in Figure 19 (iv), the vector representing $R_{-\alpha_{w,e}^+}(m_{w,e}^+)$ can be any vector ending in the interior of the second quadrant. It follows that the vectors representing all three of $m_{v,e}^-$, $m_{v,e}^+$ and $R_{-\alpha_{w,e}^+}(m_{w,e}^+)$ are in the open half-plane to the left of the y -axis.

The other four cases in the top row of Figure 2 are similar to the above case, and we omit the details. \square

Prior to the proof of Theorem 16, we have the following remark about a median in a triangle; Part (1) of the remark can be verified using Calculus, and Part (2) follows from Part (1).

Remark 17. Let σ be a triangle with vertices a , b and v , and with median from b to the opposing edge, and let δ be the angle between this median and the edge with vertices b and v , as seen in Figure 20. Let α be the angle at v , and let r_a and r_b denote the lengths of the edges from v to each of a and b , respectively. Suppose that $\alpha < \frac{\pi}{2}$.

- (1) If $r_a = r_b$, then the largest possible value of δ is $\frac{\pi}{6}$, which occurs only when $\alpha = \frac{\pi}{3}$.
- (2) If $r_a < r_b$, then $\delta < \frac{\pi}{6}$.

\diamond

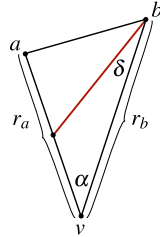


FIGURE 20.

Proof of Theorem 16. The proof starts by taking $\text{star}(v, K)$, cutting along the edges containing the vertex, and then flatten out the star into the plane, so that the chosen orientation of $\text{star}(v, K)$ corresponds to the orientation of \mathbb{R}^2 , where we recognize that there might be gaps or overlaps among the triangles with simplex-arrows after flattening, and that the order of the triangles might not be preserved; we call this flattened star B , where we continue to use v to denote the common vertex of B . The key observation is that for each edge e in $\text{star}(v, K)$ that contains v , we can determine if the pair v and e is admissible, and if yes we can compute $\beta_{v,e}$, using the triangles in B rather than the triangles in $\text{star}(v, K)$, where the difference is that in B , we rotate triangles around v by whatever angle is needed so that the edge on the counterclockwise side of one triangle lines up with the edge of the

counterclockwise side of the other triangle, and we then proceed exactly as before. It follows that we can compute the index of v using B rather than $\text{star}(v, K)$, where the clockwise tile list around v in B is the same as the clockwise tile list around v in $\text{star}(v, K)$, which is $[a_1, a_2, \dots, a_p]$.

We observe that B consists of an ordered list $\sigma_1, \dots, \sigma_p$ of acute triangles with simplex-arrows in the plane, where (1) all the triangles in the list intersect in the vertex v , and (2) for each $i \in \{1, \dots, p\}$, the edge containing v on the clockwise side of σ_i has the same length as the edge containing v on the counterclockwise side of σ_{i+1} , where addition is mod p . We call any such configuration of triangles in plane a **broken fan with simplex-arrows**. See Figure 21 for an example of a broken fan with simplex-arrows.

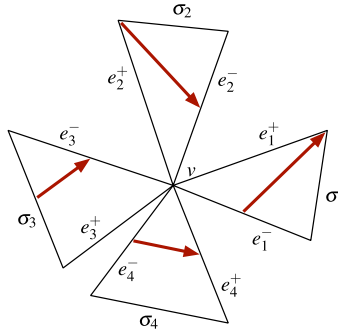


FIGURE 21.

Because ϕ is continuous, then by Remark 10 (2) we know that ϕ is admissible, and it follows that the broken fan with simplex-arrows B is also admissible, in the sense that it is admissible at every edge that contains v .

Let \mathcal{A} denote the space of all admissible broken fans with simplex-arrows in \mathbb{R}^2 with p triangles and with clockwise tile list $[a_1, a_2, \dots, a_p]$. We observe that the function that takes each broken fan with simplex-arrows in \mathcal{A} and assigns its index at v is a continuous function. Because this function has integer values, it follows that it is constant on each component of \mathcal{A} . Hence, the theorem will be proved if we can continuously deform the original broken fan with simplex-arrows B into another broken fan with simplex-arrows E that has all equilateral triangles, where the deformation stays in \mathcal{A} .

We now assume without loss of generality that the common vertex v of the broken fan with simplex-arrows B is at the origin. Let W be the set of all the vertices of all the triangles of B , excluding v . We will deform B by moving the vertices in W , and keeping v fixed at the origin. The details of the deformation, which has two parts, will be given below, where our work consists of showing that the triangles in B are always acute and that B is always admissible throughout the deformation.

For the first part of the deformation, let C_1, C_2, \dots, C_m be the partition of W into those subsets of vertices that are equidistant to the origin, where the vertices in C_1 are tied for being the farthest from the origin among all the vertices in W , all the vertices in C_2 are tied for being the second farthest from the origin among all the

vertices in W , and so on. For each $i \in \{1, \dots, m\}$, all the vertices in C_i are on a circle centered at the origin.

The first part of the deformation is done in steps, where for the first step, we move all the vertices in C_1 uniformly towards the origin, stopping when these vertices are in C_2 ; all the vertices in W other than those in C_1 do not move during this step. We claim that throughout this step of the first part of the deformation, all triangles remain acute, and admissibility is preserved.

For acuteness, let a and b be vertices in W that together with v form a triangle in B . There are three cases to consider. First, suppose that $a, b \in C_1$, in which case this triangle stays similar to itself throughout this step of the deformation, and so acuteness is preserved. Second, suppose that $a, b \notin C_1$, in which case this triangle is unchanged throughout this step of the deformation, and so acuteness is preserved. Third, suppose that $a \in C_1$ and $b \notin C_1$; reversing the roles of a and b is similar, and we omit that case. There are now two subcases, depending upon whether $b \in C_2$ or not, where if not then b is closer to the origin than C_2 , by the definition of C_2 ; see the two parts of Figure 22. We consider the first subcase; the second subcase is similar, and we omit the details. We know that at the start of this step of the deformation the point b is closer to the origin than a , and hence, the angle at a is smaller than the angle at b . At the end of this step of the deformation the point a will be in C_2 , and so a stays farther from the origin than b except at the end of the deformation, at which point a and b are equidistant from the origin, and so throughout this step of the deformation, the angle at b gets smaller, and the angle at a gets larger, where the angle at a stays less than the angle at b except at the end of the deformation, at which point the angles at a and b will be equal. Given that the angles at a and b were originally less than $\frac{\pi}{2}$, it follows that that will still be the case throughout this step, so that acuteness is preserved.

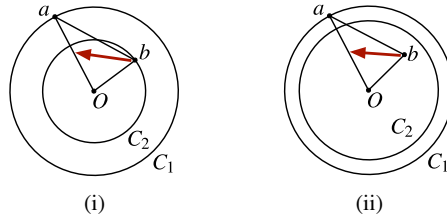


FIGURE 22.

To show that admissibility is preserved, recall that by Theorem 11, we know the 32 simple allowable adjacencies in Figure 16 are always continuous, because the triangles stay acute throughout this step, and hence they are admissible throughout this step as well. Moreover, it can be verified that a down-sink and an up-source are also always admissible (though not always continuous), using the same type of argument used in the proof of Theorem 11; we omit the details. By contrast, a down-source and an up-sink are not in general always admissible (as can be seen from a variation of Figure 12), but we now show that in the present context admissibility is preserved for any down-source; up-sinks are similar, and here too we omit the details.

Suppose that for some $i \in \{1, \dots, p\}$, the triangles σ_{i-1} and σ_i of B form a down-source, as seen in Figure 23; let angles δ_i^- , δ_i^+ and α_{i-1} be as seen in the figure. To show that admissibility is preserved for this edge throughout this step of the first part of the deformation, we need to verify that $R_{\alpha_{i-1}}(m_{i-1})$ and m_i are not negative multiples of each other throughout this step of the deformation. Because ϕ is continuous, we know that for the initial broken fan with simplex-arrows B , the three vectors representing m_{i-1} , m_i and $R_{\alpha_{i-1}}(m_{i-1})$ are contained in an open half-plane. It follows that at the start of this step of the deformation, we have $\delta_i^- + \delta_i^+ + \alpha_{i-1} < \pi$. To verify that admissibility is preserved throughout this step, it will suffice to verify that $\delta_i^- + \delta_i^+ + \alpha_{i-1} < \pi$ holds throughout this step.

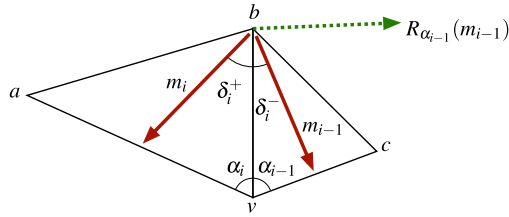


FIGURE 23.

Clearly α_{i-1} does not change throughout this step of the deformation. There are now six cases to consider. First, suppose that $a, b, c \in C_1$, in which case both triangles stay similar to themselves throughout this step of the deformation, and so δ_i^- and δ_i^+ are unchanged. Second, suppose that $a, b, c \notin C_1$. Then throughout this step of the deformation, in which case both triangles are unchanged, and so are δ_i^- and δ_i^+ .

Third, suppose that $a, b \in C_1$ and $c \notin C_1$, seen in Figure 24 (i); reversing the roles of a and c is similar, and we omit that case. When a and b are moved closer to the origin, we see that the triangle containing these two vertices stays similar to itself, and so δ_i^+ is unchanged. By Remark 17 (1), we know that $\delta_i^+ \leq \frac{\pi}{6}$ throughout. At the same time, it is clear that δ_i^- increases, but by Remark 17 (1) and (2) we see that $\delta_i^- \leq \frac{\pi}{6}$ throughout this step of the deformation. Given that $\alpha_{i-1} < \frac{\pi}{2}$, it follows that throughout this step of the deformation, we have $\delta_i^- + \delta_i^+ + \alpha_{i-1} < \frac{\pi}{6} + \frac{\pi}{6} + \frac{\pi}{2} < \pi$.

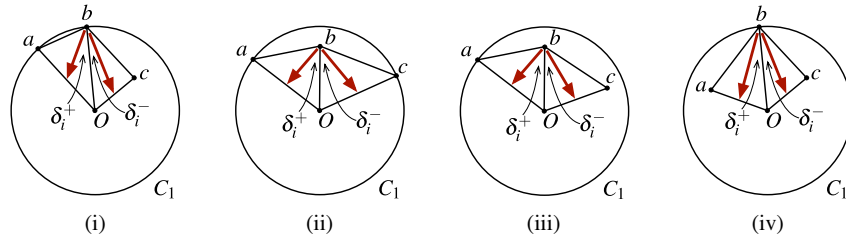


FIGURE 24.

Fourth, suppose that $a, c \in C_1$ and $b \notin C_1$, as in Figure 24 (ii). In this case, when a and c are moved closer to the origin, it is clear that both δ_i^+ and δ_i^- decrease throughout this step of the deformation, and hence so does $\delta_i^- + \delta_i^+ + \alpha_{i-1}$; because

$\delta_i^- + \delta_i^+ + \alpha_{i-1} < \pi$ at the start of this step of the deformation, the inequality holds throughout.

Fifth, suppose that $a \in C_1$ and $b, c \notin C_1$, as in Figure 24 (iii), or that the roles of a and c are reversed. This case is similar to the fourth case, and we omit the details.

Sixth, suppose that $b \in C_1$ and $a, c \notin C_1$, as in Figure 24 (iv). This case is similar to the third case, and we omit the details.

For the second step of the first part of the deformation, we move all the vertices in C_2 (including those formerly in C_1) uniformly towards the origin, stopping when these vertices are in C_3 ; all the vertices in W other than those in C_2 do not move during this step. The same argument used in the first step shows that in this step too acuteness and admissibility are preserved. We then move all the vertices in C_3 uniformly to C_4 , and so on, until all the vertices are in the circle C_m .

For the second part of the deformation, we take each triangle, which is now isosceles, and we move its vertices other than v , staying on the circle C_m , so that if the angle at v is larger than $\frac{\pi}{3}$, then the vertices should be moved closer to each other until the angle at v equals $\frac{\pi}{3}$, and if the angle at v is smaller than $\frac{\pi}{3}$, then the vertices should be moved farther apart from each other until the angle at v equals $\frac{\pi}{3}$. Clearly acuteness is preserved throughout this part of the deformation. By Remark 17 (1), we know that $\delta_i^+ \leq \frac{\pi}{6}$ and $\delta_i^- \leq \frac{\pi}{6}$ throughout this part of the deformation. Given that $\alpha_{i-1} < \frac{\pi}{2}$ throughout this part of the deformation, it follows that $\delta_i^- + \delta_i^+ + \alpha_{i-1} < \frac{\pi}{6} + \frac{\pi}{6} + \frac{\pi}{2} < \pi$ throughout. \square

REFERENCES

- [Ban67] Thomas Banchoff, *Critical points and curvature for embedded polyhedra*, J. Diff. Geom. **1** (1967), 245–256.
- [Ban70] ———, *Critical points and curvature for embedded polyhedral surfaces*, Amer. Math. Monthly **77** (1970), 475–485.
- [Blo98] Ethan D. Bloch, *The angle defect for arbitrary polyhedra*, Beiträge Algebra Geom. **39** (1998), 379–393.
- [CMS84] J. Cheeger, W. Muller, and R. Schrader, *On the curvature of piecewise flat spaces*, Commun. Math. Phys. **92** (1984), 405–454.
- [DO11] Satyan L. Devadoss and Joseph O’Rourke, *Discrete and computational geometry*, Princeton University Press, Princeton, NJ, 2011.
- [Fed82] P. J. Federico, *Descartes on Polyhedra*, Springer-Verlag, New York, 1982.
- [Hop26] Heinz Hopf, *Vektorfelder in n-dimensionalen Mannigfaltigkeiten*, Math. Ann. **96** (1926), 225–250.
- [Kni12] Oliver Knill, *A graph theoretical Poincaré-Hopf theorem*, 2012, <https://arxiv.org/abs/1201.1162v1>. arXiv:1201.1162v1 [math.DG].
- [Mil65] John W. Milnor, *Topology from the differentiable viewpoint*, University Press of Virginia, Charlottesville, VA, 1965. Based on notes by David W. Weaver.
- [Mor29] Marston Morse, *Singular points of vector fields under general boundary conditions*, Amer. J. Math. **51** (1929), 165–178.

- [Poi85] Henri Poincaré, *Sur les courbes définies par les équations différentielles (troisième partie)*, Journal de mathématiques pures et appliquées **4** (1885), 167–244.
- [Pug68] Charles C. Pugh, *A generalized Poincaré index formula*, Topology **7** (1968), 217–226.
- [Sch91] Marie-Hélène Schwartz, *Champs radiaux sur une stratification analytique*, Travaux en Cours [Works in Progress], vol. 39, Hermann, Paris, 1991 (French).
- [Sea08] Christopher Seaton, *Two Gauss-Bonnet and Poincaré-Hopf theorems for orbifolds with boundary*, Differential Geom. Appl. **26** (2008), no. 1, 42–51.
- [Spi99] Michael Spivak, *A Comprehensive Introduction to Differential Geometry*, 3rd ed., Vol. 1, Publish or Perish, Houston, 1999.